

Paraconductivity along the a and b axes in $\text{YBa}_2\text{Cu}_3\text{O}_{7-\delta}$ single crystals

W. Holm, Yu. Eltsev, and Ö. Rapp

Department of Solid State Physics, The Royal Institute of Technology, S-100 44 Stockholm, Sweden

(Received 6 September 1994)

We have measured the resistance along the a and b axes on several untwinned single crystals of $\text{YBa}_2\text{Cu}_3\text{O}_{7-\delta}$. To extract the fluctuation part of the conductivity three methods were applied which deal with the contribution from the chains in different ways. The fluctuations along a and b were found to be roughly equal for all samples while the chain fluctuations were about half an order of magnitude smaller. For all samples and regardless of choice of analysis methods we also obtain good agreement with the three-dimensional XY model for critical fluctuations in the region close to T_c .

INTRODUCTION

The study of superconducting fluctuations in high-temperature superconductors (HTSC) is a very active field. Several attempts have been made to measure the fluctuation contribution to conductivity,¹⁻⁵ magnetization,^{3,4} and magnetoconductivity.^{6,7} The first study of paraconductivity in single crystals¹ contains references to earlier work on polycrystalline samples. Analysis of these experiments, except for magnetoconductivity, requires estimation of the normal-state properties.

In this paper we focus on the conductivity fluctuations in $\text{YBa}_2\text{Cu}_3\text{O}_{7-\delta}$ (YBCO) and report on results of resistivity measurements along the a and b directions of naturally untwinned single crystals. The atomic structure of this compound implies an anisotropy in the ab plane. This has also been observed experimentally.⁸⁻¹⁰ The common point of view is that Cu-O chains act as metallic conductors and thus do not contribute to the fluctuation conductivity.⁸⁻¹⁰ Here we find that there are superconducting fluctuations in the chains but that they are about half an order of magnitude smaller than the fluctuations in the planes.

The sensitivity of high- T_c superconductors to impurities and stoichiometry raises the question if and how such defects influence the fluctuation analyses. Furthermore, due to the poor knowledge of the normal state, it is not straightforward to deduce these fluctuations from the measured resistivity. This is particularly true for the b axis, where the controversial question of the chain contribution to the conductivity presents difficulties.

We have dealt with these problems in the following way. By studying several samples, common features in the fluctuations can be identified, which are independent of the slightly varying properties between samples. We present results for seven independent measurements along the a and b axes for different samples of $\text{YBa}_2\text{Cu}_3\text{O}_{7-\delta}$. For the b -axis fluctuations we employ three different methods of analysis based on different assumptions of how to treat the chain contribution to the conductivity. These analysis will be described below. Some differences between samples and different methods of analysis are found, in particular, concerning the temperature range of normal-state fits. Nevertheless, for all samples and all methods of analysis, we find roughly the

same magnitude of the fluctuations along the a - and b -axis directions and a critical fluctuation region with an exponent p in $\Delta\sigma \sim T^p$ of $p \approx -\frac{1}{3}$ up to about 0.02 in reduced temperature $\ln(T/T_c)$.

EXPERIMENTAL TECHNIQUES

YBCO single crystals were grown using the self-flux method.¹¹ Approximately 1 g of $\text{YBa}_2\text{Cu}_3\text{O}_{7-\delta}$ was crushed and dissolved at a temperature of 1000°C in the ratio 1:6.5 in a mixture of BaO and CuO (28–72 mol %). This charge was allowed to cool slowly in a Y_2O_3 stabilized ZrO_2 crucible in a horizontally directed temperature gradient of about 5–7°C/cm. At the bottom of the crucible about 20 free-standing crystals could be recovered. The crystals were further annealed for a few days at 460°C in oxygen in order to optimize the oxygen content. Some of the crystals were found to be untwinned when examined under polarized light. The approximate sizes were $0.5 \times 0.1 \times 0.01$ mm³.

Electrical contacts were prepared by applying strips of silver paint, followed by heat treatment in flowing oxygen at 460°C for 1 h. We used a four-probe in-line contact arrangement. The size of the contacts were of the order 0.05×0.1 mm². In one case (sample No. n501) it was possible to put eight contacts on one crystal, thus enabling direct measurement in both the a and b directions on the same crystal. In another case (sample No. n1000) a crystal was cut in two untwinned pieces, one along a and one along b , from one crystal, again making measurements in two directions possible.

The resistance was measured with a standard four-probe method using a digital multimeter (Solartron SB7081) with thermal compensation. The measuring current was 1 mA with a corresponding sensitivity of 10 $\mu\Omega$. The temperature was monitored using a calibrated Pt resistor with a maximum error of ± 50 mK and a relative accuracy of ± 0.5 mK.

Because of the large contact sizes, as compared to the sample dimensions, accurate determination of the resistivity was difficult. Therefore we fixed the resistivity at 100 K to the mean values of our measurements, i.e., 100 $\mu\Omega$ cm for ρ_a and 60 $\mu\Omega$ cm for ρ_b . These values are on the high side within previous reports.^{9,10,12} The T_c 's of our crystals were in the range 91–92 K with transition

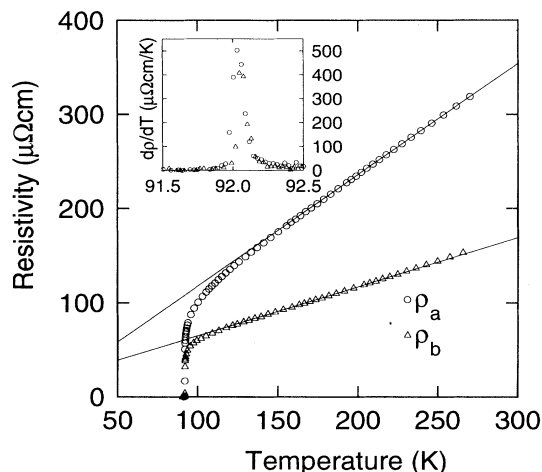


FIG. 1. Resistivities along a and b of an untwinned single crystal (sample No. n1000). The solid lines are linear fits to the data. Shown in the inset are the derivatives used for determining T_c .

widths of approximately 0.2 K. T_c was defined as the inflection point of the R -vs- T curve. Shown in Fig. 1 are the transition curves for a typical sample together with an inset showing how T_c was determined.

METHODS OF ANALYSIS

The methods of analysis were the following.

(i) The traditionally accepted way to estimate the normal-state resistivity in HTSC is to fit a straight line at high temperatures and extrapolate it to low temperatures. The fluctuation conductivity $\Delta\sigma_i$ is then extracted from the measured ρ_i by

$$\Delta\sigma_i = \frac{1}{\rho_i} - \frac{1}{\rho_i^n}, \quad (1)$$

where i is the a or b direction and n denotes the normal state.

(ii) From the crystallographic structure it is tempting to assume that the Cu-O chains act as one-dimensional conductors, thus contributing only to the b -axis conductivity. A simple model has been suggested^{9,10,12} to consider the a -axis resistivity equal to the resistivity of the Cu-O₂ planes, and the resistivity along b as a parallel circuit between chains and planes. The chain resistivity

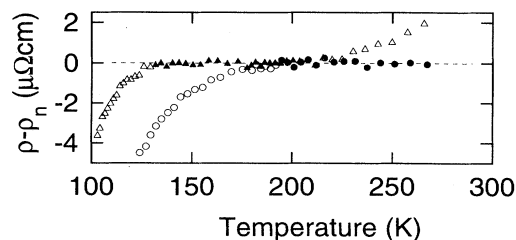


FIG. 2. Difference between the estimated normal states along a (circles) and b (triangles) for a typical crystal. The solid symbols were used to define the normal state.

ρ_{chain} can then be calculated from the measured ρ_a and ρ_b by

$$\rho_{\text{chain}} = \frac{\rho_a \rho_b}{\rho_a - \rho_b}. \quad (2)$$

ρ_{chain} is fitted in the normal state to a second-order polynomial, and in the fluctuation region $\Delta\sigma$ is obtained from the difference between the calculated chain contribution and the extrapolated polynomial.

(iii) Using the functional form for the chain resistivity obtained in (ii), we can alternatively calculate the b -axis resistivity, again considering ρ_b to result from a parallel circuit of chains and planes.

$$\rho_b^n = \frac{\rho_{\text{plane}}^n \rho_{\text{chain}}^n}{\rho_{\text{plane}}^n + \rho_{\text{chain}}^n}, \quad (3)$$

where ρ_{plane}^n is assumed equal to ρ_a^n . The fluctuation contribution is now obtained from Eq. (3) and the measured ρ_b by

$$\Delta\sigma_b = \frac{1}{\rho_b} - \frac{1}{\rho_b^n}. \quad (4)$$

RESULTS

To determine the normal states in the methods described above, we fitted the assumed functional dependences to the part of the resistivity curve where no noticeable deviation was found. This is illustrated for method (i) in Fig. 2. All results have been collected in Table I together with the temperature intervals used.

TABLE I. Overview of the samples studied and the different normal states.

Sample	Measured along	T_c (K)	ρ_n ($\mu\Omega$ cm) (with T in K)	ρ_n defined from (see Fig. 2)
twb1	b	92.02	$6.6 + 0.58T$	$140 < T < 180$
twb2	b	91.28	$1.7 + 0.65T$	$140 < T < 200$
twa2	a	91.73	$13.5 + 1.05T$	$T > 205$
n1000	a	92.03	$-0.8 + 1.18T$	$T > 200$
n1000	b	92.05	$12.5 + 0.52T$	$130 < T < 210$
n1000	chain		$140 + 0.0022T^2$	$T > 170$
n1000	chain		$93.4 + 0.46T + 0.0011T^2$	$T > 100$
n501	a	91.84	$35.1 + 0.73T$	$T > 200$
n501	b	91.86	$23.2 + 0.38T$	$150 < T < 200$
n501	chain		$130 + 0.0021T^2$	$T > 100$

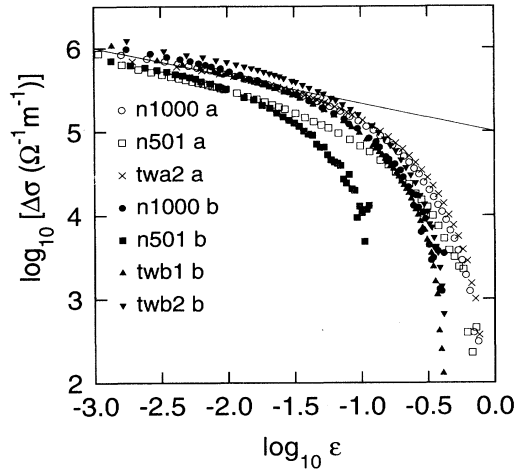


FIG. 3. The fluctuation contribution to the conductivity along a and b for several untwinned single crystals as obtained from Eq. (1). Solid symbols are used for b -axis fluctuations and open symbols and crosses for the a axis. The straight line has the slope $-1/3$, which should describe critical conductivity fluctuations in the 3D XY model.

When applying method (i) above we found that a straight line could be fitted to ρ_a above about 200 K. For ρ_b , on the other hand, clear deviations from linearity were observed at higher temperatures, and successful fitting was possible only over a limited temperature range, about 150–200 K (see also Fig. 2 and the inset of Fig. 4 below). Extrapolating these linear fits and using Eq. (1), we obtain $\Delta\sigma$, which is plotted vs $\epsilon = \ln(T/T_c)$ on a log-log scale in Fig. 3. Evidently there is good agreement between different samples and the fluctuations along a and b are of the same magnitude. There is however a general trend for the fluctuations along a to persist to higher temperatures than those along b .

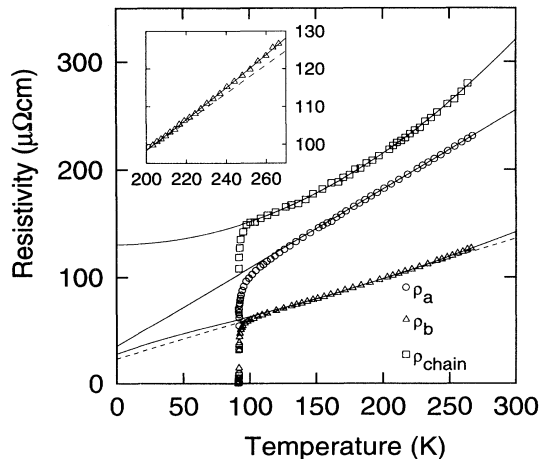


FIG. 4. The resistivities along the a and b axes and the resistivity along the chains calculated with Eq. (2) for sample No. n501. The curves are the fitted normal states. For the b axis the dashed line is a linear approximation and the full line was calculated from Eq. (3). The inset shows an enlargement for the b axis at high temperatures.

For the two crystals that were measured along both a and b , we calculated the chain resistivity using Eq. (2). Shown in Fig. 4 are ρ_a , ρ_b , and ρ_{chain} for one single crystal. To estimate the normal-state resistivity of the chains, we assumed a second-order polynomial. For one of the crystals (sample No. n501), the temperature dependence was found to be purely quadratic above 100 K. The other crystal (sample No. n1000) exhibited this behavior only above 170 K. If, however, a term linear in T was included, successful fitting down to 100 K was possible. The corresponding fluctuation conductivities for both analyses are plotted as filled and open squares in Fig. 5. For both samples it can be seen that the chain fluctuations are about half an order of magnitude smaller than the fluctuations in the planes, i.e., along a , which are plotted as circles. One may also note that the chain fluctuations for the two samples coincide well when the same temperature interval is used for defining ρ_{chain}^n albeit the functional forms of the normal states are different.

The fluctuations along b were calculated using method (iii) above and are plotted as down triangles in Fig. 5. For

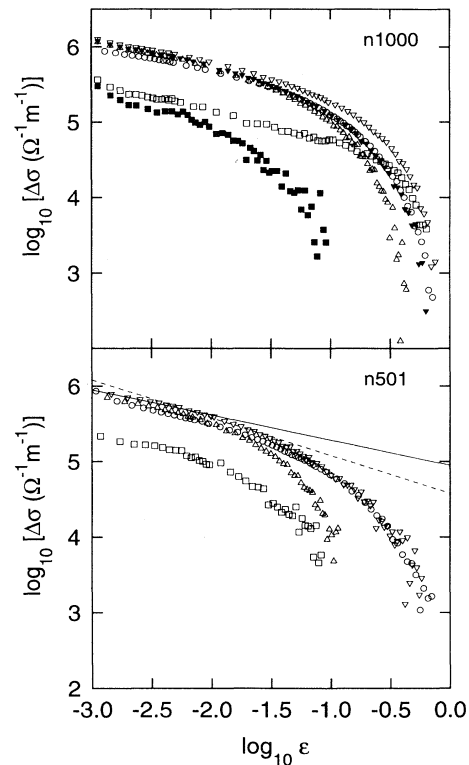


FIG. 5. Fluctuation conductivity for two crystals. The circles are for fluctuations in the planes, i.e., along a . The squares are for fluctuations along the chains. The triangles are for fluctuations along the b axis, upturned assuming a linear normal state and downturned with a normal state calculated from the fits to chain and plane resistivity [Eq. (3)]. For sample No. n1000, we defined the normal state of the chains in two ways, with and without a T -linear term. The corresponding fluctuations are shown as solid and open symbols, respectively. The full line in the lower panel has the slope $-1/3$ as predicted by the 3D XY model. The dashed line has the slope $-1/2$ illustrating the three-dimensional mean-field result.

sample No. n1000 there are two possibilities for ρ_{chain}^n in Eq. (3) corresponding to second-order polynomials with or without a term linear in T . These results are plotted in the upper panel of Fig. 5. For both samples and analysis methods the fluctuations along b calculated from Eq. (4) follow closely those along a in contrast to $\Delta\sigma$ at large ϵ in Fig. 3. It can also be noted that the normal state defined in this way describes the data better at higher temperatures than the linear fit used in method (i), as illustrated in the inset of Fig. 4.

DISCUSSION

Obviously there are some sample-dependent differences in our observations, see e.g., Fig. 3. Furthermore, depending on the chosen analysis of the normal states, the high-temperature behavior can be different, as illustrated in the inset of Fig. 4. If we employ the simple picture of a parallel circuit between planes and chains, we can show that the chain resistivity is well described by a second-order polynomial. In one case (sample No. n501) the temperature dependence was purely quadratic. Such a dependence was also reported in Ref. 12. The difference between sample Nos. n501 and n1000 in this respect is not understood.

Nevertheless, we are able to draw some general conclusions. The magnitude of the conductivity fluctuations are roughly the same along a and b . This is approximately valid for all samples in the linear analysis (Fig. 3), and it is also observed in the rather different analyses (iii) (Fig. 5). The magnitude of the fluctuations along the chains are also roughly the same for both samples (Fig. 5) and about half an order of magnitude smaller than the fluctuations in the planes.

Another important common feature for all samples and analysis methods is the slope of $\Delta\sigma$ at low ϵ . In all cases we find $\Delta\sigma \sim \epsilon^{-1/3}$ from the lower limit of the measurements of $\epsilon \approx 0.001$ to about $\epsilon = 0.02$. The full straight lines in Fig. 3 and in the lower panel of Fig. 5 illustrate this critical behavior. It is consistent with the three-dimensional (3D) XY model¹³ close to the critical point. Further support for this model is obtained from measurements of the penetration depth¹⁴ and the heat capacity.¹⁵

In this case the critical region would extend to about 1.8 K above T_c . The width estimated from the Ginzburg criterion is about 0.1 K,¹³ but according to Ref. 16 this is an underestimate by a factor of 25. Support for this argument can be found in studies of the specific heat.¹⁵

However, according to the XY model, $\Delta\sigma$ should display a crossover from an exponent $-1/3$ to $-2/3$ in the critical region before reaching the three-dimensional mean-field exponent of $-1/2$. This is not observed. The dashed line in Fig. 5 illustrates the mean-field result, and it can be seen that there is a smooth crossover between the exponents $-1/3$ and $-1/2$ in a narrow temperature region around $\epsilon = 0.02$. Similar observations have been made for the a -axis fluctuations previously,² with an exponent $-1/3$ in the critical region and no indication of an intermediate temperature region with a different critical exponent.

ACKNOWLEDGMENTS

This work has been supported by the Swedish Superconductivity Consortium and by the Göran Gustafsson Foundation.

-
- ¹T. A. Friedmann, J. P. Rice, J. Giapintzakis, and D. M. Ginsberg, *Phys. Rev. B* **39**, 4258 (1989).
²A. Pomar, A. Díaz, M. V. Ramallo, C. Torrón, J. A. Veira, and F. Vidal, *Physica C* **218**, 257 (1993).
³C. Torrón, A. Díaz, A. Pomar, J. A. Veira, and F. Vidal, *Phys. Rev. B* **49**, 13 143 (1994).
⁴U. Welp, S. Fleshler, W. K. Kwok, R. A. Klemm, V. M. Vinokur, J. Downey, B. Veal, and G. W. Crabtree, *Phys. Rev. Lett.* **67**, 3180 (1991).
⁵W. Lang, G. Heine, P. Schwab, X. Z. Wang, and D. Bäuerle, *Phys. Rev. B* **49**, 4209 (1994).
⁶W. Holm, M. Andersson, Ö. Rapp, M. A. Kulikov, and I. Makarenko, *Phys. Rev. B* **48**, 4227 (1993).
⁷J. Sugawara, H. Iwasaki, N. Kobayashi, H. Yamane, and T. Hirai, *Phys. Rev. B* **46**, 14 818 (1992).
⁸G. W. Crabtree, W. K. Kwok, U. Welp, A. Umezawa, K. G. Vandervoort, S. Fleshler, J. Downey, Y. Fang, and J. Z. Liu, in *Proceedings of the International Workshop on Electronic*

- Properties and Mechanisms in High- T_c Superconductors, Tsukuba, 1991*, edited by T. Oguchi, K. Kadowaki, and T. Sasaki (North-Holland, Amsterdam, 1992), p. 193.
⁹T. A. Friedmann, M. W. Rabin, J. Giapintzakis, J. P. Rice, and D. M. Ginsberg, *Phys. Rev. B* **42**, 6217 (1990).
¹⁰U. Welp, S. Fleshler, W. K. Kwok, J. Downey, Y. Fang, G. W. Crabtree, and J. Z. Liu, *Phys. Rev. B* **42**, 10 189 (1990).
¹¹D. L. Kaiser, F. Holtzberg, B. A. Scott, and T. R. McGuire, *Appl. Phys. Lett.* **51**, 1050 (1987).
¹²R. Gagnon, C. Lupien, and L. Taillefer, *Phys. Rev. B* **50**, 3458 (1994).
¹³C. J. Lobb, *Phys. Rev. B* **36**, 3930 (1987).
¹⁴S. Kamal, D. A. Bonn, N. Goldenfeld, P. J. Hirschfeld, R. Liang, and W. N. Hardy, *Phys. Rev. Lett.* **73**, 1845 (1994).
¹⁵G. Mozurkewich, M. B. Salamon, and S. E. Inderhees, *Phys. Rev. B* **46**, 11 914 (1992).
¹⁶D. S. Fisher, M. P. A. Fisher, and D. A. Huse, *Phys. Rev. B* **43**, 130 (1990).